Stratosphere temperature measurement using Raman lidar

Philippe Keckhut, M. L. Chanin, and A. Hauchecorne

Temperature measurements using vibrational Raman scattering from molecular nitrogen were performed simultaneously with temperature obtained by Rayleigh scattering in the amplitude range between 12 and 30 km. The downward extension of the Rayleigh temperature described in this paper leads to the possibility of obtaining a continuous temperature profile from 12 to nearly 100 km. The temperature profiles have been obtained using an instrument made up basically as a Rayleigh lidar with an extra channel. The measurements are in close agreement with the CIRA model and simultaneous balloon sounding. *Key words:* Stratosphere, Raman lidar, temperature.

I. Introduction

The concept of using molecular density measurements to derive temperature profiles has been widely used in both passive and active sounding of the atmosphere. Since June 1980, Chanin and Hauchecorne have measured, on a continuous basis, temperature from 30 to 90 km at the Observatoire de Haute Provence (OHP) in France by using a Rayleigh lidar.[1,2] However, accurate temperature measurements could not be made below ~30 km as the scattered echo cannot be assumed to be only due to Rayleigh scattering. This lower level corresponds to the top of the dust layer which can rise significantly after major volcanic eruptions. Below this altitude the scattering comes both from molecules and aerosols, and to separate the contribution of the molecular density requires a multiwavelength lidar,[3] with some assumptions about the aerosol characteristics. We show in this paper that it is possible to extend the temperature profiles downward using vibrational Raman scattering from molecular nitrogen (N_2 thereafter) with an instrument built basically like a Rayleigh lidar.

When the atmosphere is illuminated with a high powered laser, it is possible to obtain the frequency shifted backscattered radiation of the Raman component. The specific shift of the scattered radiation

frequency depends only on the vibrational levels of the molecular species.[4] For this reason the Raman lidar has been studied and used by many researchers to identify specific atmospheric components for pollutant detection. Leonard[5] first reported the observation of Raman scattering from N_2 in the atmosphere and many publications reported the observations of other species as molecular oxygen, water vapor, and many others.[6,7] Previous experiments have reached an altitude range of only a few kilometers which is satisfactory for pollutant studies. The weak efficiency of the Raman process presents considerable experimental difficulty for long range detection. The cross section of the Q-branch vibrational Raman transition in molecular gases in 3 orders of magnitude smaller than the Rayleigh cross section, but the density is 3 orders of magnitude greater at 30 km than at 80 km. Thus, theoretically the use of Raman backscattering seems to be able to provide temperature profiles up to 30 km. We choose to use the backscatter signal of the Raman vibrational levels of N_2 since its mixing ratio is known to be constant and the product of its density (78% of the molecular density) with its Raman cross section[8,9] ($4.4 \cdot 10^{-31}$ cm^2 sr^{-1} at 514.5 nm) is the largest among all the atmospheric constituents. The Raman echo, occurring at the shifted frequency, is proportional to the N_2 density and thus to the air density.

Using Raman scattering to provide temperature profiles was suggested and discussed by several authors but has never been pushed far enough to become operational with such a height range: a correlation of nearly 0.8 was previously obtained between the Raman scattering of N_2, obtained with a lidar, and the temperature measured by thermistors 30 m above ground, indicating that a Raman lidar could measure temperature fluctuations.[10] More recently Moskowitz et al.[11]

presented preliminary data of Raman measurements to examine the possibilities of self-normalizing the atmospheric density obtained by Rayleigh lidar below 30 km.

II. Description of the Lidar System

The emitted laser wavelength is chosen outside any absorption bands or resonance lines and should be as close as possible to the blue side of the spectrum. The optimum choice of the emitted wavelength is the result of a compromise between the Rayleigh and Raman cross-sectional efficiencies (varying as 1^{-4}), the atmospheric and optical transmissions, the available energy per pulse, and the repetition rate that modern lasers are able to provide. In the work reported here, the eavelength of the emitted radiation is the second harmonic (532 nm) of a Nd:YAG laser. The emission of the Raman backscatter radiation shifted for the 2331-cm^{-1} Q-branch vibrational transition of molecular N_2 gas occurs at a wavelength of 607 nm.

The total backscatter echo is collected by a telescope with a large enough field of view to obtain a geometric form factor equal to unity from 10 to 100 km.[12] The aperture located in the focal plane which defines the field of view could cut off part of the signal when the scattering volume cannot be assumed to be at infinity. The coaxial configuration used in this experiment helps to eliminate the problems of parallax and misalignment due to the large height range covered. An optical dichroic mirror is used to separate the two channels: from the first one, the Rayleigh signal at 532 nm provides the temperature measurement between 30 and 90 km (as in the Rayleigh lidar operational use), and from the other one, the Raman backscattered echo at 607 nm completes the temperature profile downward. Each signal is filtered through a narrowband filter of ~1-nm bandwidth to eliminate the sky background and is then detected by a photomultiplier followed by a pulse counting system (Fig. 1). The few percent of Rayleigh backscatteing not eliminated by the dichroic mirror is 1 or 2 orders of magnitude greater than the Raman signal. But this Rayleigh noise becomes <1 ‰ after the interference filter which has a rejection coefficient of 10^5.

III. Description of the Method

Since the Raman backscatter echo is the sole result of the N_2 density, the number of detected Raman photons per laser pulse is given by

$$N(z_i) = \frac{N_0 G A K R_q T_1 T_2 n_{N_2}(z_i) \beta_{N_2} \Delta z}{4\pi(z_i - z_0)^2},$$

where $N(z_i)$ is the number of detected photons from a layer of thickness Dz centered at height z_i, N_0 is the number of emitted photons per laser pulse, A is the telescope area, G is the geometric form factor (equal to 1 for a perfect optical alignment), R_q is the quantum efficiency of the photomultiplier, K is the optical transmission of the instrument, T_1 and T_2 are the atmospheric transmissions between the altitude of the lidar site z_o and the height of the emitting layer z_i (at
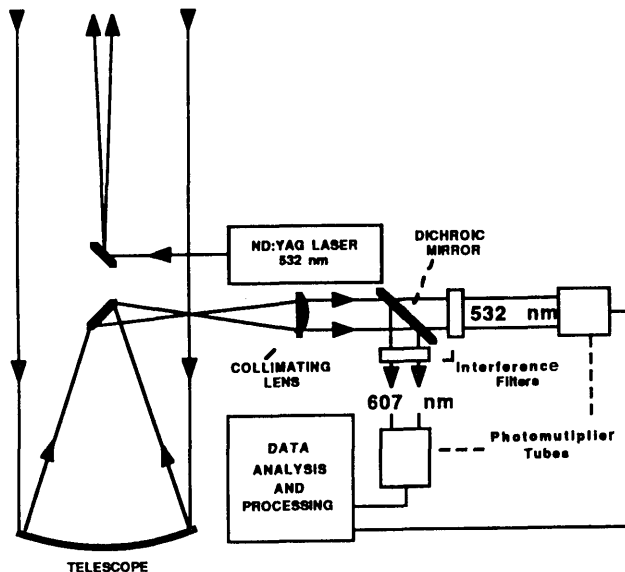

Fig. 1. Schematic diagram of the Raman–Rayleigh lidar.

both the emitted and received wavelengths), $N_{N_2}(z_i)$ is the N_2 molecular concentration, and b_{N_2} is the Raman backscatter cross section.

From the above equation, the density profile can be deduced and, as the N_2 mixing ratio is constant, the relative air density can be obtained by using the technique described by Chanin and Hauchecorne[2] for Rayleigh scattering leading to an absolute temperature determination. The temperature profile is computed from the density measurement, assuming that the atmosphere is in hydrostatic equilibrium and obeys the perfect gas law. Both signals are corrected for the nonlinearity and the dark current of the photomultipliers, the atmospheric transmission, and the sky background.

The nonlinearity is due to the fact that the Rayleigh signal, coming from lower altitudes, is large enough for the photomultiplier response to saturate in the photon counting mode. The region of overlap of the Raman and Rayleigh signals (25–35 km) is used to calculate the coefficients of the photon counting response assumed to be exponential.

The atmospheric transmission depends on Rayleigh, Mie, and ozone attenuations and cannot be assumed to be constant below 30 km. The transmission is computed using the CIRA 86 model to obtain the Rayleigh optical thickness, a model[13] for ozone attenuation, and the statistical aerosol database from the lidar measurements of OHP[14] to calculate the aerosol attenuation. Total corrections of Rayleigh, ozone, and Mie attenuations are given in Table I, in present-day conditions, expressed in temperature deviations. The total correction is ~3% at an altitude of 10 km, and a 10% uncertainty on this correction leads to a 0.3% uncertainty in temperature (<1 K) which is close to the level of the statistical noise for 1-h integration time and 300-m resolution. In fact, aerosols and ozone above 12 km do not vary much during such a short time. Below this

TABLE I. Attenuation Correction Given in Temperature Change				
Altitude km	Standard error %	Rayleigh %	Ozone %	Mie %
10	0.2	2.2	1.0	0.7
20	0.7	0.5	0.9	0.2
30	0.05	0.1	0.3	0.0

TABLE II. Lidar Characteristics

| Emitter	
Laser type	Nd:YAG
Energy per pulse	300 mJ at 532 nm
Repetition rate	30 Hz
Divergence	10^{-4} rad
Receiver	
Telescope diameter	1.20 m
Field of view	10^{-3} rad
Wavelengths	532 and 607 nm
Bandpass filters	1 nm

TEMPERATURE (KELVIN)

Fig. 2. Lidar temperature profiles compared with the corresponding CIRA 1988 model (dashed lines): (A) 09/11/88, 19H03 06H17; (B) 08/02/89, 18H26 06H13; (C) 14/04/89, 21H05 23H56.

critical height or after major volcanic periods, clouds and haze lead to an important change of the atmospheric transmission, and a better accuracy would require a better aerosol determination as discussed later. At the time of the measurements, the scattering ratio between Mie and Rayleigh was small ($R = 10\%$) and aerosols were therefore not an important source of attenuation above 12 km. Furthermore, if aerosol[14] and ozone[15] concentrations are obtained by lidar at the same place and time, as is the case at the OHP, they should be used to lead to a more accurate determination.

The noise from the sky background is constant with height and is then obtained by averaging the signal from the altitude range where the backscattered signal is negligible compared to the noise level, i.e., above 110 and 80 km, respectively, for the Rayleigh and Raman channels. The noise which could be induced by the strong echoes of the lower layers is avoided by using an electronic shutter.

Initialization of the Raman profile is done at the upper limit of the profile by using the Rayleigh profile obtained at the same time. The Raman signal is corrected by a constant normalization factor to give the same signal level as the Rayleigh one; this factor is calculated in the altitude range where both signals are available (25–35 km). This common range is limited downward at 25 km for the Rayleigh signal due to the contribution of Mie scattering by aerosols and upward at 35 km for the Raman signal by the signal-to-noise ratio, which at this level is ~30 with an integration time of 1 h and a spatial resolution of 300 m.

The theoretical ratio between the Rayleigh and Raman signals, using calculated cross sections and assuming the atmospheric transmission, optical characteristics, and N_2 density, is ~3500 which corresponds to the normalization factor obtained experimentally. A continuity in the density profile is then obtained with the Raman signal below 25 km, the Rayleigh
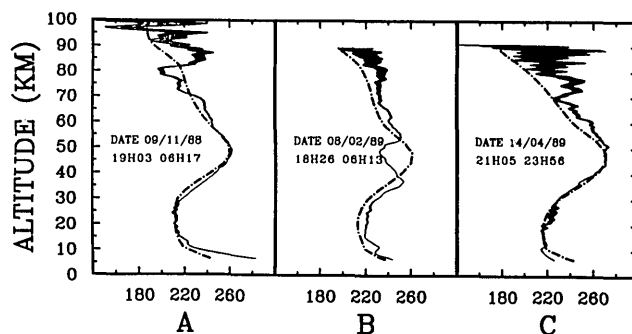
signal above 35 km, and the average of both between 25 and 35 km. The resulting signal, which extends continuously from 12 up to 90 km, is used to derive temperature as explained in previous publications.[1,2]

IV. Experimental Results

The results reported here have been obtained at the Centre d'Essai des Landes at Biscarrosse, France (CEL: 44°20′N, 1°15′W), with a lidar having the characteristics given in Table II. The choice of this site instead of our research site at OHP was made because of the coaxial structure of this lidar.

As is well known, the temperature accuracy is essentially given by the photon statistical noise and depends on the square root of the number of received photons $N(z)$. The accuracy then depends on the height and time resolutions which are chosen to maximize the backscattered signal according to the temporal and spatial scales under study. Three examples of nightly averaged temperature profiles measured with such a lidar are presented in Fig. 2. They were obtained with a vertical spatial resolution of 300 m and filtered with a five-point window numerical filter. These temperatures, extending continuously from the tropopause up to the mesopause, are compared with the CIRA 86 model of the relevant month. The standard error of the Raman part of the profile given with a 95% confidence level is better than ±1.5 K at 30 km, ±0.8 K at 20 km, and ±0.2 K at 10 km, when obtained with 12 h of integration as in case B. In that case the large difference observed between the temperature profile shown and the CIRA model near the stratopause is due to a stationary planetary wave which was present during Feb. 1989 over Western Europe. In cases A and C, the resulting profiles are in close agreement with the model.

The lower part of the three lidar observations are presented in Fig. 3 together with the nearest radiosonde profiles. Case A corresponds to the first experiment performed in the Raman mode; in that case we used, as for the Rayleigh mode, a field of view of 10^{-4} rad. As a consequence, the resulting profile shows a very large difference with the radiosonde. The calcu-
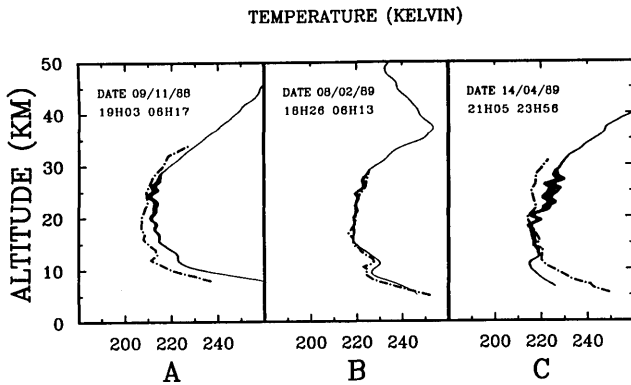
TEMPERATURE (KELVIN)

Fig. 3. Lidar temperature profiles compared with the corresponding balloon sounding obtained on (A) 09/11/88, 19H15; (B) 09/02/89, 07H30, (C) 14/04/89, 00H00.

TEMPERATURE (K)

Fig. 4. Temporal evolution during a February night with a time resolution of 1 h and a vertical resolution of 300 m.

lation of the geometric form factor.[12] for the optical parameters used for this experiment confirms that a problem of focusing would appear around 20–25 km and gain importance lower down. We then chose to use a larger field of view (10^{-3} rad) for the Raman channel and the profile shown in case B indicates that good agreement is then observed above 12 km between the lidar profile and the simultaneous radiosonde. The third example given in case C was obtained in the presence of subvisible clouds and good agreement is only obtained between 12 and 20 km. A large difference is observed below 12 km, likely because of the uncertainty in estimating the atmospheric transmission at this level. Above 20 km the difference could be attributed to the day-to-day variability (as the observations were made within one day intervals), or more likely to a misfunctioning of the radiosonde itself, as the upper part of the sounding is in large disagreement with both the model and the resulting lidar profile. One could conclude from these comparisons that, in the absence of large aerosol content, the Raman lidar can provide a reliable temperature measurement in the low stratosphere.

The presence of cirrus in the upper troposphere prevents the downward extension unless the cloud transmission can be measured. This could be obtained by measuring the scattering ratio from both the Rayleigh and Raman channels but it requires a third channel of lower senstivity for the Rayleigh to avoid the saturation of the signal. Then the ratio of the backscattered signals at 532 nm (molecules and aerosols) and 607 nm (molecular nitrogen) will provide a measurement of the scattering ratio. This provides a way to separate the Mie from the Rayleigh contribution. If the angular function of scattering is known, the ratio between the average cross section per unit of solid angle, db/dW, for 180° scattering and the total cross section b could be determined with a hypothesis on the particle size distribution.[16] The temperature profile could then be corrected from aerosol attenuation with better accuracy using Mie backscattering.[17]
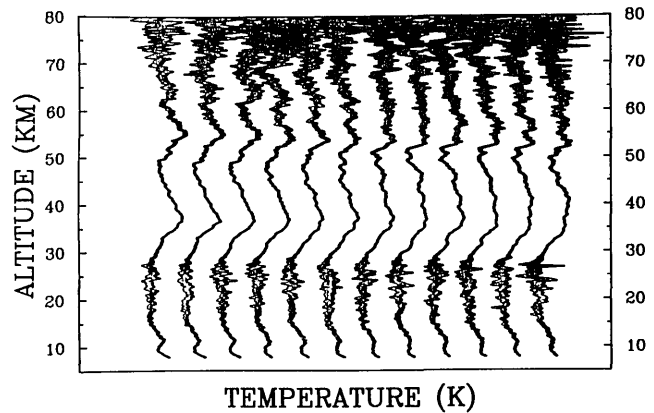
Temperature fluctuations of short periods due to

gravity waves have been detected by the Rayleigh lidar and presented in several studies above 30 km.[18,19] If the Raman profiles can be available in the low stratosphere with a time resolution of <1 h, an altitude resolution of 300 m, and an acceptable accuracy (5 K, 30 km; 2 K, 20 km; 0.5 K, 10 km), it becomes possible to extend such studies downwards (Fig. 4). More information on the characteristics of the gravity waves below 30 km could provide better insight into the relationship between the wave activity and their orographic and meteorologic sources. Gravity wave results obtained from ongoing analysis of the Raman profile in addition to the Rayleigh profile will be the subject of another paper.

V. Discussion

The quality and scientific impact of the measurements made with the Rayleigh lidar have already been demonstrated in many studies[2,18–20]; its downward extension would amplify these advantages which are mainly the following:

(1) The absolute temperature determination by lidar does not require any external calibration is not affected by instrumental drift.

(2) If the downward continuity in altitude is insured between the Rayleigh and Raman profiles, a unique instrument essentially identical to the Rayleigh lidar is sufficient for covering the whole middle atmosphere.

(3) The height and time resolution can be adequately chosen to answer the scientific needs (gravity waves, tides, planetary waves, long term variability).

(4) The mean nightly averaged temperature profile is not affected by the variability and the structures due to gravity waves which affect any individual radiosonde or rocket profile; this is important when looking for climatic trends of small amplitude.

The systematic errors and bias come mainly from four sources:

A possible parallax effect between the emission and reception axis which can be avoided by using a coaxial system and a large field of view.

The error, due to the modeled pressure value used to

initiate the temperature retrieval, is evaluated to be <15% at the top of the Rayleigh profile and it decreases rapidly with the altitude[1]; the resulting error below 70 km could be considered totally negligible and such model fitting is not required for the Raman profile.

Error due to the linearization of the photomultiplier response can be correctly evaluated in considering the coherence of both signals.

The error in evaluating aerosol and ozone attenuation was discussed earlier and can be minimized by simultaneous O_3 and aerosol measurement.

However the correction due to the aerosol attenuation may not be performed with adequate accuracy if the aerosol load in the atmosphere is too large, as after a major volcanic eruption. A scattering ratio of more than 10 has been observed with the OHP lidar after the volcanic eruption of El Chichon in summer 1982.[14] This may be the main limitation of the method.

VI. Conclusions

Comparison of temperature obtained with Raman lidar and with balloon sounding has shown that the Raman method can be used with adequate accuracy in the 10–25-km height range. This provides the possibility of obtaining a complete temperature profile of the atmosphere from the tropopause up to the mesopause with a unique instrument, operating on a continuous basis by combining Rayleigh and Raman echoes. When the technique is perfected, it could eliminate the need to launch radiosondes whenever there is special difficulty (onboard ships or during strong winds...). Furthermore, this may be a way to obtain temperature by lidar ~25–40 km when the atmosphere is distributed by volcanic dust, a situation which occurred after the El Chichon eruption up to an altitude of 38 km. The determination of the aerosol attenuation may however lead to a large uncertainty during these periods. The study of gravity waves should be possible with reasonable height and time resolutions in a height range not accessible up to now.

In the near future, with the development of more powerful lasers and multimirror receivers, the performances of the Raman lidar could be enhanced. It will allow a thorough survey in this altitude range where very accurate temperatures are required for long term monitoring of climatological changes.

References

1. A. Hauchecorne and M. L. Chanin, "Density and Temperature Profiles Obtained by Lidar Between 35 and 70 km," Geophys. Res. Lett. 7, 565–568 (1980).
2. M. L. Chanin and A. Hauchecorne, "Lidar Studies of Temperature and Density Using Scattering," Map Handbook 13, 87–89 (1984).
3. G. K. Yue, "Wavelength Dependence of Aerosol Extinction Coefficient for Stratospheric Aerosols," J. Climate Appl. Meteorol. 25, 1775–1779 (1986).
4. C. V. Raman, "A Change of Wave-Length in Light Scattering," Nature London 121, 619 (1928).
5. D. A. Leonard, "Observation of Raman Scattering From the Atmosphere Using a Pulsed Nitrogen Ultraviolet Laser," Nature London 216, 142–143 (1967).
6. J. A. Cooney, "Uses of Raman Scattering for Remote Sensing of Atmospheric Properties of Meteorological Significance," Opt. Eng. 22, 292–301 (1983).
7. S. H. Melfi, "Remote Measurement of the Atmosphere Using Raman Scattering," Appl. Opt. 11, 1605–1610 (1972).
8. W. R. Fenner, H. A. Hyatt, J. M. Kellam, and S. P. S. Porto, "Raman Cross Section of Some Simple Gases," J. Opt. Soc. Am. 63, 73–76 (1973).
9. H. A. Hyatt, J. M. Cherlow, W. R. Fenner, and S. P. S. Porto, "Cross Section for the Raman Effect in Molecular Nitrogen Gas," J. Opt. Soc. Am. 63, 1604–1606 (1973).
10. R. G. Strauch, V. E. Derr, and R. E. Cupp, "Atmospheric Temperature Measurement Using Raman Backscatter," Appl. Opt. 10, 2665–2669 (1971).
11. W. P. Moskowitz, G. Davidson, D. Sipler, C. R. Philbrick, and P. Dao, "Raman Augmentation for Rayleigh Lidar," in Abstract, Lidar International Conference (Innichen San Candido, Italy, May 1988).
12. T. Halldorsson and J. Langerholc, "Geometrical Form Factors for the Lidar Function," Appl. Opt. 17, 240–244 (1978).
13. S. L. Valley, Ed., Handbook of Geophysics and Space Environments (McGraw-Hall, New York, 1965).
14. J. Lefrere, J. Pelon, C. Cohen, A. Hauchecorne, and P. Flamant, "Lidar Survey of the Post Mt. St. Helens Stratospheric Aerosol at Haute Provence Observatory," Appl. Opt. 20, A70–1117 (1981).
15. J. Pelon, S. Godin, and G. Megie, "Upper Stratospheric (30–50 km) Lidar Observations of the Ozone Vertical Distribution," J. Geophys. Res. 8, 8667–8671 (1986).
16. M. P. McCormick, J. D. Lawrence, Jr., and F. R. Crownfield, Jr., "Mie Total and Differential Backscattering Cross Sections at Laser Wavelengths for Junge Aerosol Models," Appl. Opt. 7, 2424–2425 (1968).
17. M. Hirono and T. Shibata, "Enormous Increase of Stratospheric Aerosols Over Fukuoka Due to Volcanic Eruption of El Chichon in 1982," Geophys. Res. Lett. 10, 152–154 (1983).
18. A. Hauchecorne, M. L. Chanin, and R. Wilson, "Mesospheric Temperature Inversion and Gravity Waves Breaking," Geophys. Res. Lett. 14, 933–936 (1987).
19. R. Wilson, M. L. Chanin, and A. Hauchecorne, "Gravity Wave Spectra in the Middle Atmosphere as Observed by Rayleigh Lidar," Geophys. Res. Lett., in press.
20. M. L. Chanin, N. Smires, and A. Hauchecorne, "Long Term Variation of the Temperature of the Middle Atmosphere at Mid Latitude: Dynamical and Radiative Causes," J. Geophys. Res. 92, 933–941 (1987).